Quantitative evaluation of induced porosity reference samples implemented by drill hole in CFRP using XCT and various segmentation parameters

G. Rao[1], B. Plank[1], C. Heinzl[1] and J. Kastner[1]

[1]University of Applied Sciences Upper Austria, Austria
Email: guruprasad.rao@fh-wels.at, Web Page: http://www.fh-ooe.at

Keywords: Reference porosity, CFRP, Segmentation parameters, X-ray computed tomography

Abstract

Determination of porosity in carbon fibre reinforced polymers (CFRP) using X-ray computed tomography (XCT) is an important reference method for quality control in aerospace industry. The main objective of this work is to create reference samples of carbon fibre reinforced polymer (CFRP) and evaluate porosity quantitatively using X-ray computed tomography (XCT). Artificial porosity was induced in three non-porous CFRP laminates by multiple cylindrical holes drilled with a diameter of 200 and 300 µm. These plates were arranged in different permutations to obtain various combinations of a pre-determined void content. The combinations of CFRP plates were scanned using XCT for porosity determination. The diameters of the drilled cylinders implanted were measured with voxel size of 5 μm^3 XCT scans with an accuracy of 295 ± 2.75 µm and 196 ± 2.75 µm to obtain reference porosity limits. The reference samples results show a void content ranging from 0.96 up to 4.81vol. %.
Voxel variation scans (VVS) were performed for a reference sample with 4.52 ± 0.07 vol. % of porosity from $(11\ \mu m)^3$ to $(120\ \mu m)^3$ voxel sizes to obtain comparative results of various global thresholds as well as visualize acceptable air-material boundary segmentation. Voxel size (VS) of $(11\mu m)^3$ was identified as an optimum resolution for these purposes and sample size. Five global threshold methods were investigated for segmentation and results were compared. A novel segmentation method was introduced from the adaptation of ISO50 threshold. The adapted method from ISO50 threshold led to results within the expected porosity range. It provided accurate porosity results for macro voids with smallest individual void volume above $30\times10^6\ \mu m^3$ in CFRP. We show that the selection of a global threshold at an optimum resolution is very important in determination of porosity quantitatively in CFRP material system.
The repeatability of the experiment was performed by scanning a reference sample with 4.4 ± 0.07 vol. % of porosity at optimum resolution of $(11\ \mu m)^3$ voxel size to consider variations in sample preparation, measurements and evaluation uncertainties. The standard deviation in porosity volume evaluated with ISO50 adapted thresholds were within ± 0.03 vol. % showing reasonable reproducibility.

1. Introduction and motivation

Carbon fiber reinforced polymers (CFRP) are primarily used in aeronautical, automotive and aerospace applications due to its excellent properties such as light-weight, high specific stiffness, high specific strength, excellent fatigue resistance, outstanding corrosion resistance, the ability to fabricate directional mechanical properties and high dimensional stability [1]. However, the introduction of porous structures or voids during the manufacturing stages reportedly deteriorates the mechanical and physical properties of CFRP. Experiments carried out by Sergio Almeida and Zabulon Neto to assess the effect of void content on static strength and fatigue life of composite laminates under flexural loading indicated that voids have a strong detrimental effect on composite structures [2]. The experiments conducted by Bhat et al shows the drastic drop in interlaminar shear strength (ILSS) as the void content goes beyond 2 vol. % [3].
Different non-destructive methods have been studied in literature such as active thermography, microwave testing, eddy currents, magnetic particles, ultrasonic testing (UT), X-ray computed tomography which evaluate porosity with varied resolution and have different sensitivity. The

Excerpt from ISBN 978-3-00-053387-7

current standard procedure in aeronautical industry for evaluating the porosity in carbon composites is using ultrasound attenuation (UT) [4]. The error margin evaluated by E A Birt and R A Smith while evaluating porosity in CFRP with the help of ultrasound (UT) was up to ± 0.5 vol. %. [5]. It indicates correct interpretation of UT evaluation also depends on experience and expertise of the inspector. Evaluations performed by Ciliberto et al. comparing infrared and ultrasound methods also indicate that the evaluation and interpretation of results depends on expertise and experience of the inspector [6]. For this reason, X-ray computed tomography (XCT) is an ideal supplementary 3D reference method. In addition, with advanced XCT devices resolution down to < 1 µm can be achieved to provide detailed information regarding shape and location of the void [7].

X-ray computed tomography is in use since late 1970s prominently in non-invasive medical diagnostics. Use of X- rays for 3D imaging of materials started from late 1990s with the introduction of industrial computed tomography systems [8]. The fast improvement in detector hardware and simultaneous amelioration of acquisition and reconstruction software has made industrial computed tomography (XCT) a very robust and reliable tool in the sector of non-destructive testing and analysis. The primary principle of XCT is acquisition of attenuated X-rays passed through a target object-of-interest mounted on a rotary table rotated at an equal angular rotation of 360 degrees and subsequently reconstructing the images using reconstruction software to obtain 3-D information of inner structures. Various attempts have also been made using different software algorithms to characterize and segment the voids present in CFRP during manufacturing stages. The porosity maps with an interactive exploration and visual analysis of porosity in CFRP quantifies an industrial CFRP specimen [9]. The MObjects is a method for the visualization and interactive exploration of defects in XCT Data is where every pore is analysed based on a set of properties such as volume, shape factor and desired number of classes [10].

The primary aim of this experiment is to artificially induce pre-determined voids (porosity) in non-porous samples and evaluate the porosity using different segmentation methods. This experiment also tries to find out deviation in porosity by performing repeatability experiments to establish a standard to measure porosity for the given material system and parameters.

2. Experimental Setup

The CFRP sample investigated in our work consists of 5 plies of PREPREG C 970/PWC T300 3K UT (TY) in plain weave style. In the case of a non-porous material it consists of 60 wt. % carbon fibres and 40 wt. % epoxy resin. The average density of the samples was measured at 1.56 ± 0.03 g/cm^3. The single prepreg ply thickness for industrial porosity samples was 0.2159 mm. A total of five samples each with five ply thickness were selected for our investigations. Three samples namely D1, D2 and D3 were drilled using 200 µm and 300 µm holes. Two samples were kept non-porous and marked as NP1 and NP2 respectively. Figure 1shows the drilled samples D1, D2 and D3.

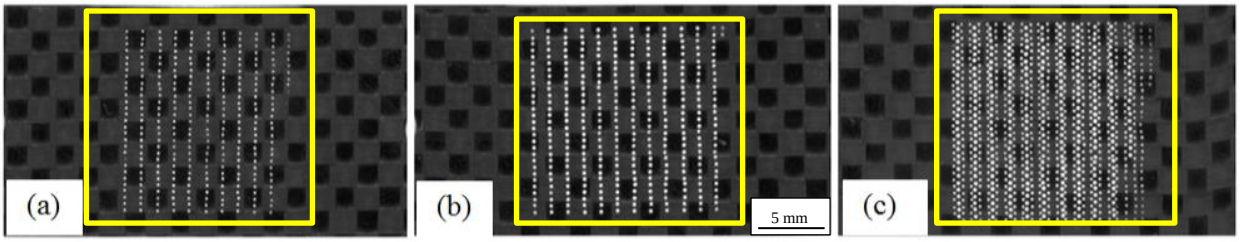

Figure 1 CFRP samples with drilled holes (a) Sample D1 (b) Sample D2 (c) Sample D3 [11]

Excerpt from ISBN 978-3-00-053387-7

The diameters of the drilled cylinders with 300 µm and 200 µm implanted were measured at scans with voxel size of 5 μm^3 XCT scans at an accuracy of 295 ± 2.75 µm and 196 ± 2.75 µm respectively [11]. The expected porosity limits for our experiment were calculated based upon total volume of all cylinders obtained after considering maximum deviation from these evaluated XCT cylindrical diameters.

Table 1 Number of artificially induced porosity drill holes in every sample plate

Ply	Holes drilled	Diameter of drill	Ideal cylindrical volume of single drill hole intra-ply
NP1, NP2	0	--	
D1	300	200 µm	3.141×10^7 μm^3
D2	350	300 µm	7.060×10^7 μm^3
D3	1,010 (310 and 700)	200 and 300 µm	

The samples were then layered in various combinations as shown in Table 2. The expected porosity range is also shown for every combination. Thin filler material layers of less than 100 µm width having X-ray absorption slightly lower than the CFRP material were inserted between the plates to reduce a probable air gap. The expected porosity range was evaluated after measuring drill hole diameters with XCT scanned at voxel size of $(5\ \mu m)^3$ [11]. The volume region of interest for analysis was defined by using the adaptive rectangle tool from VGStudio MAX 2.2 software from Volume Graphics GmbH. For voxel variation scans it was implemented using a square measured at 17×17 mm in front view and software adapted boundary based on depth 2 and grey value 32800 in top view as shown in Figure 2.

Table 2 Various combinations of drilled samples and layer sequence of sample plates [11]

	Layer sequence	**Expected Porosity Range (vol. %)**
Combination I	NP1-D1-D2-D3-NP2	4.81 ± 0.12
Combination II	NP1-D1-NP2	0.96 ± 0.02
Combination III	NP1-D2-NP2	2.58 ± 0.03
Combination IV	NP1-D3-NP2	4.52 ± 0.07

2.1 X-ray Computed Tomography and XCT Data Analysis Software

XCT scans were performed on a Nanotom 180 NF device manufactured by GE phoenix|x-ray. The device uses a 180 keV nano-focus tube and a 2304² pixel flat panel detector (Hamamatsu). Molybdenum was used as target material. No pre- or post-filters were used for the scans. The applied voltage on the X-ray tube was 60 kV at a voxel size between $(11\ \mu m)^3$ and $(120\ \mu m)^3$. Voxel sizes were calibrated using a 3.9796 ± 0.0020 mm ball bar manufactured by GE. The reconstruction was performed using datos|x-reconstruction software from GE using filtered back projection algorithm. Evaluations were done using VGStudio MAX 2.2 software [12] and our in-house tool iAnalyse [13] developed by the University of Applied Sciences Upper Austria. 32 to 16 bit grey value mapping was done manually by calculating the values semi-automatically. The XCT scans performed at the same sample with the same parameters except varying voxel size of the scans. This is referred to as voxel variation scans (VVS).

Excerpt from ISBN 978-3-00-053387-7

3. Results

As the Combination IV shows the drill holes with both 200 and 300 µm diameters, voxel variation scans (VVS) were performed at the voxel sizes of 11, 22, 30, 40, 44, 60, 80 and 120 µm^3. Figure 2 (a) shows the front view and (b) the top view of Combination I along the volume of interest marked with cyan using adaptive rectangle algorithm to remove the surrounding air, (c-i) shows the unsegmented and ISO50 segmented drilled holes at various voxel sizes after surface determination for the zoomed region in red boundary. It can be seen that air-material boundary is most prominently differentiated at 11 µm^3 voxel size. As voxel size increases the boundary becomes progressively blurred. Beyond 60 µm^3 the void resolution reduces drastically up to a point where at VS 120 µm^3 nearly no voids are detected with ISO50 threshold. The total volume of region of interest is the volumetric region of the sample which is considered for analysis excluding the surrounding air. This is implemented for our sample in VGStudio MAX 2.2 using an adaptive region of interest (ROI) tool by first defining a fixed area in the front view with edge of the square within a symmetrical sample and then extending these lines in top view which automatically adapts to the boundary between external material surface and surrounding air.

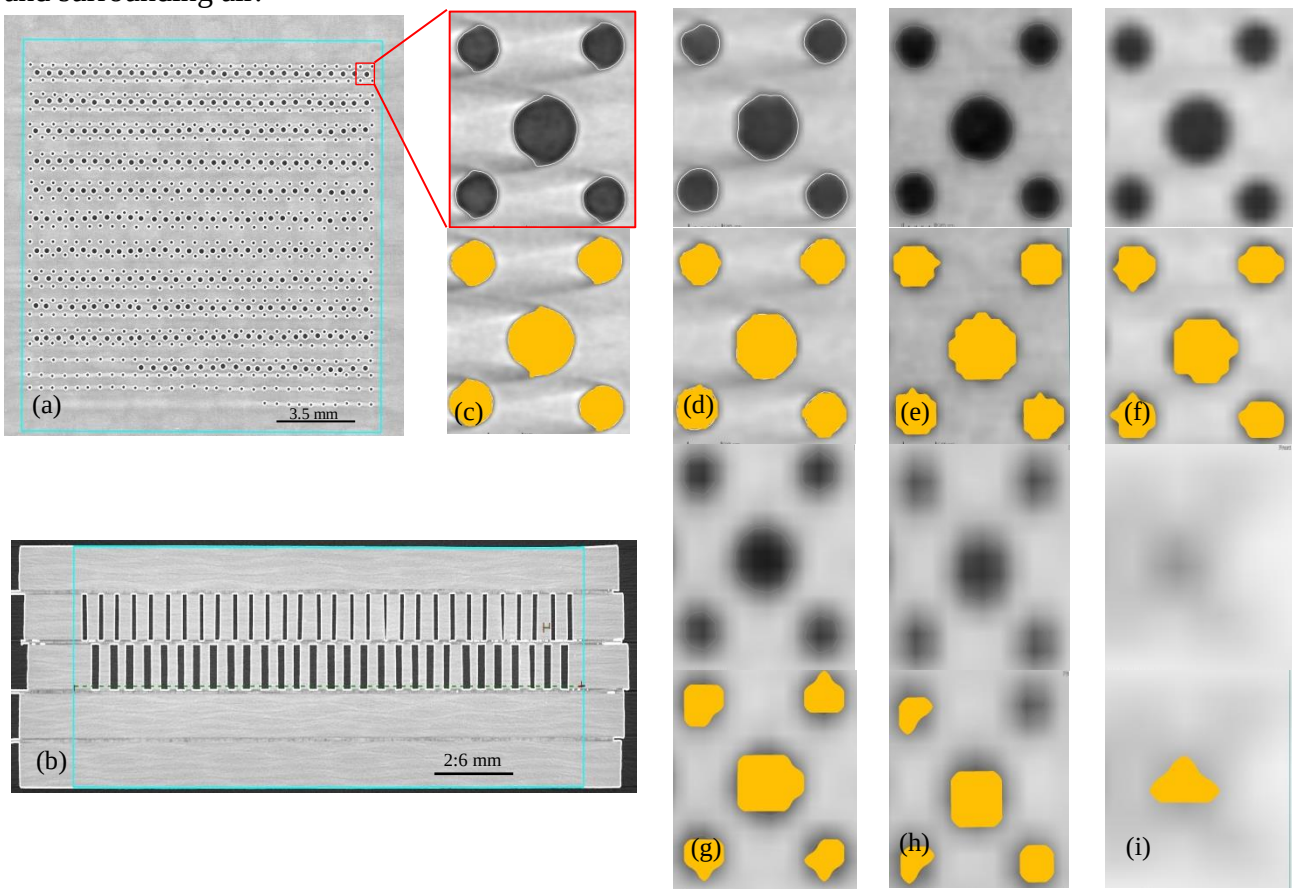

Figure 2 (a) Front view Combination I Plate D3 at 11 µm; cyan lines indicating volume region of interest 17 × 17 mm (b) Top view Combination I at 11 µm; cyan lines indicating volume region of interest determined based on adaptive rectangle associated with end points marked in front view (c-i) zoomed in region of red square displaying voxel variation scans (VVS) for samples at voxel sizes (c) 11 µm^3 (d) 22 µm^3 (e) 30 µm^3 (f) 40 µm^3 (g) 60 µm^3 (h) 80 µm^3 (i) 120 µm^3 with top unsegmented and bottom ISO50 segmented.

These scans were evaluated for volume porosity using five global thresholds methods, namely Airbus threshold [14], Airbus adapted threshold [15], ISO50 threshold, Maximum Distance threshold (MaxD) [16] [17] and OTSU threshold [18] respectively. Figure 3 shows the porosity

Excerpt from ISBN 978-3-00-053387-7

percentage by volume of the CFRP samples at various voxel sizes for various global thresholds evaluated using defect detection tool from VGStudio MAX 2.2 at constant minimum volume (CV) of 27,000 µm^3. The expected porosity for the Combination IV was 4.52 ±0.07 vol. % as represented by min and max lines in Figure 3. Airbus and MaxD thresholds give largest deviation from the expected porosity limits. At 120 µm^3 VS all the thresholds provide results with highly over-segmented values. OTSU shows a consistent over segmentation of around 0.3 to 0.5 percentage points from 11 to 44 µm^3 suddenly decreasing at 60 µm^3. Porosity volume detected by ISO50 threshold gives closest values from 11 µm^3 to 30 µm^3 but decreases by 1 percentage point from 30 to 80 µm^3. Airbus adapted threshold shows under segmentation at 11 µm^3 and consistently shows a slight over-segmentation at higher voxel sizes.

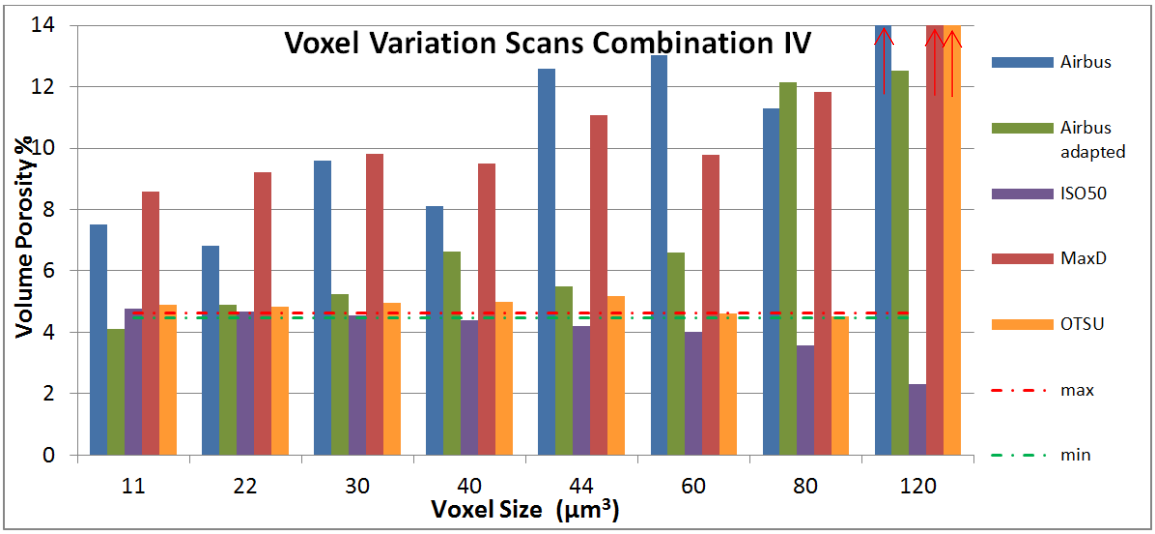

Figure 3 Voxel variation scan results for Combination III

The ISO50 threshold was found to be very robust at voxel sizes from (11 µm)^3 to (30 µm)^3 with porosity results within ± 0.5 vol. % of expected porosity limits. To obtain an improved performance of ISO50 threshold; a novel way was devised to observe the variation in porosity determined at varied equi-distant grey values. This was implemented by evaluating the complete range of grey values by fixing the end points at air peak and material peak. ISO50 was defined as a point at 50 % of this range, ISO45 as the 45 % of this range, ISO65 as 65 % and a similar nomenclature was followed where ISOXX was used to define a robust global ISO threshold with XX being the percentage range of grey value at which the global ISO threshold was fixed. Figure 4 shows a bi-modal grey value histogram of Combination I scanned at (11 µm)^3 voxel size. X-axis shows the grey value and Y-axis represents frequency of grey values of voxels observed in the scanned data. The maximum grey value peak for air and material is depicted along with equi-distant ISOXX grey value thresholds in Figure 4.

Excerpt from ISBN 978-3-00-053387-7

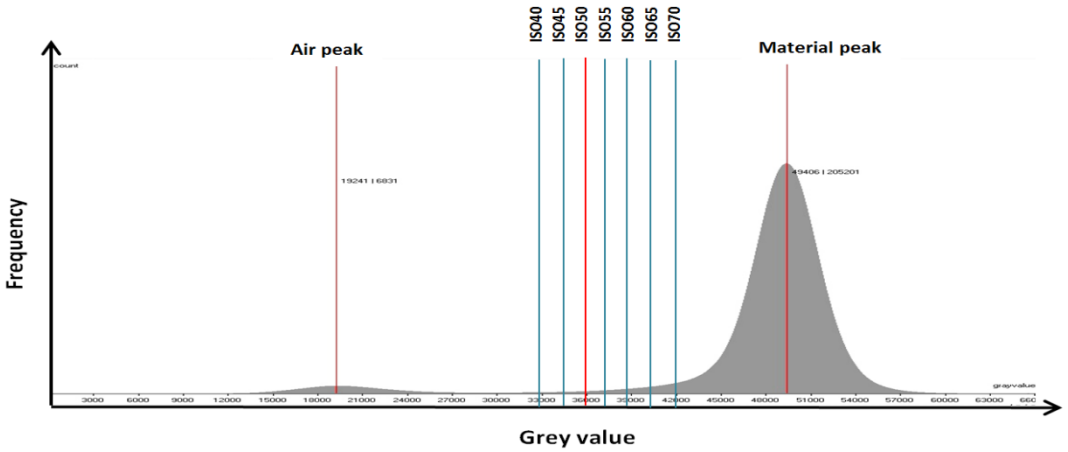

Figure 4 Bi-modal grey value histogram of Combination I at (11 µm)^3 voxel size and determining grey values for ISOXX global segmentation threshold

Figure 5 shows the results for volume porosity at voxel sizes ranging from (11 µm)^3 to (120 µm)^3 evaluated with increasing ISO levels of 5 percent points from ISO45 up to ISO70 for Combination I. It can be seen that as the voxel size increases, the volume porosity for the thresholds ISO45, ISO50 and ISO55 decreases whereas for the thresholds ISO60, ISO65 and ISO70 the volume porosity increases. The decrease in porosity at lower ISO thresholds is due to the under-segmentation of certain voxels. The increase in porosity at higher ISO thresholds is the result of segmentation of filler material.

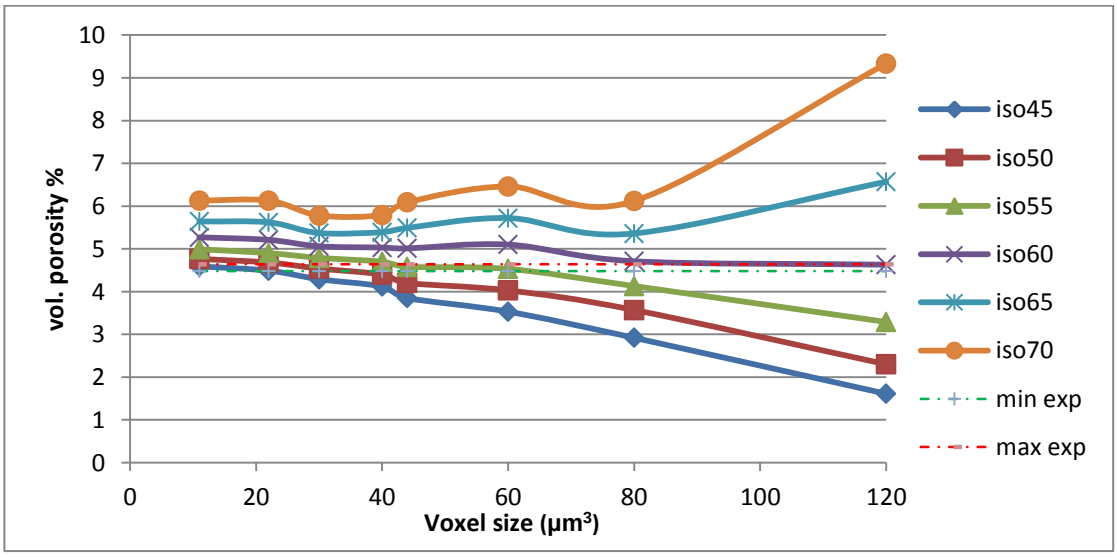

Figure 5 Volume porosity evaluation using ISO variation thresholds at various voxel sizes

Also, a consistent over-segmentation was observed at lower voxel sizes for ISO60 and above at all voxel sizes. A detailed porosity evaluation using ISO variation is contained in Figure 6. Figure 6 (a) depicts ISO variation results for ISO45, ISO50 and ISO55 as only these thresholds cross the expected porosity limits at lower voxel sizes. Furthermore it was also shown that from ISO45 to ISO50 the detected porosity volume was very close to the expected values of porosity. Figure 6 (b) depicts the evaluation of a single percent point increasing ISO threshold from ISO45 to

Excerpt from ISBN 978-3-00-053387-7

ISO50. It can be observed that porosities extracted with ISO45, ISO46 and ISO47 remain within the porosity limits from 11 to 25 µm^3. ISO49 and ISO50 are within the range of expected porosity at a comparatively higher voxel sizes from 25 to 30 µm^3. At (11 µm)^3 voxel size the volume porosity detected at ISO46 returned 4.62 vol. % which is well within limits up to the voxel size of (25 µm)^3.

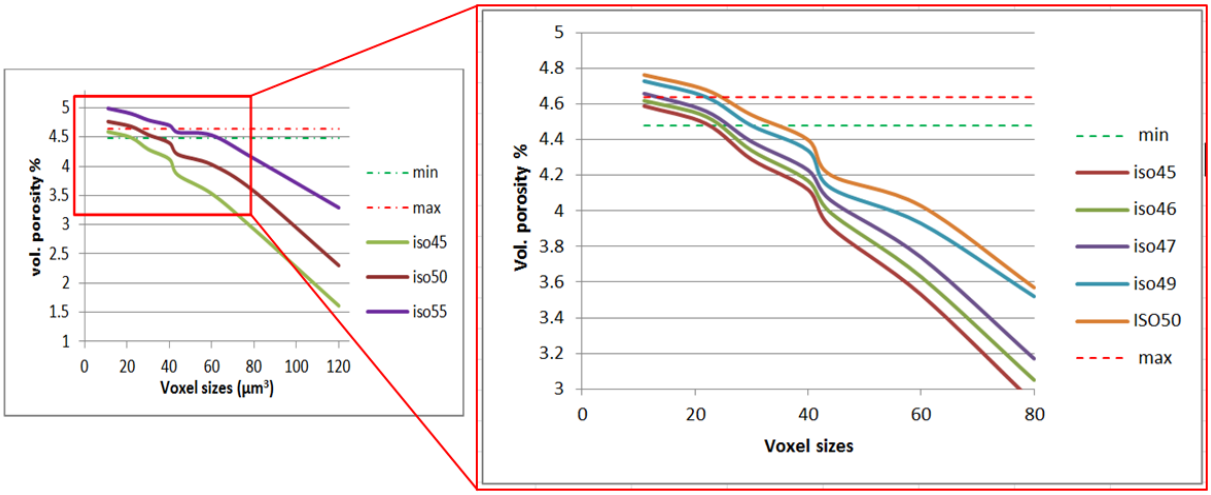

Figure 6 (a) Detailed view of ISO variation for ISO45, ISO50 and ISO55 (b) singular percentage point incremental ISO variation from ISO45 to ISO50 for Combination IV

3.1 Experiments for repeatability of the evaluations

The repeatability and reproducibility of the experimental results was checked by performing five scans at (11 µm)^3 voxel size for Combination I. The CT parameters used for measurement of repeatability analysis are mentioned in Table 3 (a). The described values are voltage (U in kV), current (I in µA), integration time (T in milli-seconds), voxel size (µm^3), number of projection images (N proj.). The repetitive scans iterations were named ITR-1, ITR-2, ITR-3, ITR-4 and ITR-5. The entire sample was disassembled and regrouped in a different layered sequence prior to each scan as shown in Table 3 (b).

Table 3 (a) Constant Scan parameters for repeatability analysis (b) Combinations of sample plates at various iterations during repeatability experiments.

U	60 kV
I	310 µA
T	600 ms
VS	11 µm^3
N proj.	1700

Iteration 1 (ITR-1)	NP1-D1-D2-D3-NP2
Iteration 2 (ITR-2)	NP1-D3-D1-D2-NP2
Iteration 3 (ITR-3)	NP2-D3-D-2D1-NP1
Iteration 4 (ITR-4)	NP2-D1-D3-D2-NP1
Iteration 5 (ITR-5)	NP1-D2-D1-D3-NP2

The scans were performed within a time interval of 2 weeks to consider measurement uncertainties in parameters due to changes in surrounding conditions apart from scan parameters. The scans were performed with the exactly same scan parameters including source-object distance and source-detector distance to obtain a constant magnification and voxel size. The volume region of interest for the repeatability analysis was also defined by using the adaptive rectangle tool from VGStudio MAX 2.2. It was implemented using a square measured of 17×18.5 mm in front view and software evaluated adapted boundary with depth 2 and grey value

Excerpt from ISBN 978-3-00-053387-7

set at ISO55 in top view. The expected porosity range was evaluated at 4.40 ± 0.07 vol. %. The mean ROI volume measured by VGStudio MAX 2.2 was 1.62×10^{12} µm^3. The standard deviation for the total ROI volume for ITR-1 to ITR-5 was evaluated at ± 0.516 vol. %. As the combinations evaluated had non-porous samples at outer periphery in all the scan iterations as shown in Table 3 (b), the effect of the deviation in ROI is only on the total volume and not on volume of the voids detected. The standard deviation in detected volume porosity due to variation in total ROI volume was evaluated at ± 0.02 vol. %. The reproducibility of the experiment evaluating volume porosity at various ISOXX thresholds, Airbus adapted threshold and OTSU threshold can be seen in Table 4. The maximum standard deviation in all the repeatability scans for detected volume porosity by ISOXX methods was ± 0.03 vol. %. This result corroborates with the porosity evaluation of real porosity samples in [17] and shows that the results are reasonably accurate. The maximum standard deviation in the porosity results was observed for Airbus adapted threshold at ± 0.14 vol. %. Figure 7 depicts the results for repeatability analysis for five iterations at ISO45, ISO50, OTSU and Airbus adapted threshold along with minimum and maximum expected porosity limits. It was also observed that ISO45 gave porosity results closer to the lower end of the expected porosity limits whereas ISO50 gave porosity results slightly higher to the upper maximum limit for all the iterations. This implies that the exact porosity could be evaluated by implementing global threshold slightly more than ISO45 (for eg. ISO46).

Table 4 Table showing percentage volume porosity evaluated at different global thresholds as a part of reproducibility tests on Combination I at 11 µm^3 voxel size for five set of scanned dataset.

	ISO40	ISO45	ISO50	ISO55	ISO60	OTSU	Airbus adapted
ITR-1	4.41	4.52	4.65	4.84	5.11	4.75	4.61
ITR-2	4.49	4.6	4.72	4.88	5.08	4.78	4.74
ITR-3	4.45	4.57	4.71	4.88	5.09	4.78	4.97
ITR-4	4.48	4.58	4.7	4.85	5.05	4.73	4.74
ITR-5	4.44	4.55	4.69	4.86	5.08	4.73	4.67
Standard deviation	0.03	0.03	0.03	0.02	0.02	0.03	0.14

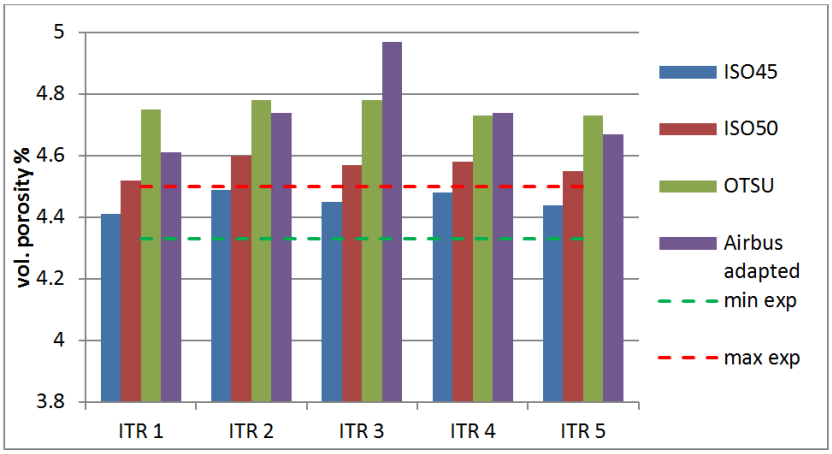

Figure 7 Results for Repeatability analysis for five iterations evaluated at 11 µm^3 voxel size

Excerpt from ISBN 978-3-00-053387-7

4. Discussions

The optimum segmentation threshold in conformity with XCT scan method should be derived in a way that following requirements are fulfilled:

1. It should be easy and fast to calculate and implement for porosity evaluation.
2. The segmentation threshold must give porosity within the range at lower voxel sizes where the void-material boundary is clearly visible. In this case $(11\ \mu m)^3$ was found to be suitable after voxel variation scan examinations.
3. The segmentation threshold must provide consistent results with least standard deviation when constant scan parameters such as kV, µA, voxel size are fixed during XCT scan.
4. The segmentation threshold should provide results within the stipulated porosity limits.
5. The porosity limits should be standardised with XCT high resolution scans evaluations.
6. The prior calibration of the metrology of voxel size must be performed using standardised methods such as ball-bar method and the results should be implemented by over-riding the voxel dimensions in the subsequent scans.
7. The segmentation threshold evaluation should not depend on any other material system except the material under consideration for porosity evaluation.

As **ISO46** satisfies all of the above criteria, it is an optimum global segmentation threshold for our induced reference porosity CFRP samples. The maximum standard deviation in the repeatability scans for detected volume porosity by ISOXX methods was ± 0.03 vol. %. This indicates good reproducibility of results for porosity using XCT modality.
Although computed tomography has evident manifold advantages in porosity evaluation, certain challenges of measurement on macro and micro levels need to be considered. On macro level, there is an inherent limitation on the maximum size of the sample which can be scanned with decreasing voxel sizes in order to achieve higher resolutions. The total scan time for the acquisition is dependent on the number of projection images to be acquired. The total scan time for each iteration scan (ITR-1 to ITR-5) was 130 minutes. The reconstructed data obtained have file sizes of up to 12 GB for a 32-bit data and 6 GB for a 16-bit data. It highlights the need of having state of the art multi-tasking and multi-processing work stations and large data storage capabilities. On micro level the challenges deal with evaluation intricacies. There is a deviation of ± 0.03 vol. % on porosity value due to deviation of up to $1\times10^{10}\ \mu m^3$ in total volume of region of interest. Despite certain advantages of the filler material such as separation of individual cylindrical structures, reduction of inadvertent air gap between samples and providing lower grey values for the evaluation of airbus adapted threshold which unequivocally help the measurement, it also induces some limitations as it gets segmented at the higher ISOXX thresholds resulting in higher porosity.
In future, the evaluated porosity using optimum resolution and adapted thresholds can be applied for lower resolution and larger sample sizes for this material system after extrapolating the results from voxel variation scans.

5. Summary and Conclusions

In our work there were challenges on two levels. One was to implant a known amount of separate and measurable voids. Second was to validate the various known segmentation methods for their accuracy and repeatability. A pre-determined porosity from 0.96 to 4.48 vol. % was constructed using various combinations of drilled samples. The Combination IV which had porosity of 4.52 ±0.07 vol. % was specifically scanned from 11 μm^3 to 120 μm^3 voxel sizes and evaluated using

Excerpt from ISBN 978-3-00-053387-7

five global segmentation thresholds to observe the accuracy of these methods and to provide results within expected limits. ISO50 was found to be a robust segmentation threshold. A novel segmentation method ISOXX was developed based on ISO50 to achieve porosity within expected limits with high repeatability. To test the repeatability of results five scans were performed on Combination I with expected porosity limits of 4.40 ± 0.07 vol. %. The results obtained were reproducible with maximum standard deviation in measurement of ± 0.03 vol. % for all ISOXX thresholds. The ISO46 was found to be an optimal global threshold for our induced porosity reference CFRP sample evaluations. These results show that X-ray computed tomography is a very powerful tool for non-destructive quantification of volumetric porosity in artificially induced reference CFRP samples. It can be further used in scientific and industrial non-destructive testing laboratories as an additional reference method for porosity evaluation in composites.

Acknowledgements

This work was financed by the K-Project ZPT+ supported by COMET programme of FFG and by the federal government of Upper Austria and Styria. Furthermore, we wish to thank FACC AG and TU-Vienna for manufacturing the CFRP specimens. The research leading to these results has also received funding from the European Union's Seventh Framework Programme (FP7/2007-2013) under grant agreement No. 607817 (INTERAQCT: International Network for the Training of Early stage Researchers on Advanced Quality control by Computed Tomography).

References

[1] L. Tong, A. P. Mouritz und M. Bannister, „3D fibre reinforced polymer composites," Elsevier, 2002.

[2] S. F. M. de Almeida und Z. d. S. N. Neto, „Effect of void content on the strength of composite laminates," *Composite structures,* Bd. 28, Nr. 2, pp. 139-148, 1994.

[3] M. Bhat, M. Binoy, N. Surya, C. Murthy und R. Engelbart, „Non-destructive evaluation of porosity and its effect on mechanical properties of carbon fiber reinforced polymer composite materials," 2012.

[4] „Methods and apparatus for porosity measurement and defect detection". #sep#~9 2014.

[5] E. Birt und R. Smith, „A review of NDE methods for porosity measurement in fibre-reinforced polymer composites," *Insight-Non-Destructive Testing and Condition Monitoring,* Bd. 46, Nr. 11, pp. 681-686, 2004.

[6] A. Ciliberto, G. Cavaccini, O. Salvetti, M. Chimenti, L. Azzarelli, P. Bison, S. Marinetti, A. Freda und E. Grinzato, „Porosity detection in composite aeronautical structures," *Infrared physics \& technology,* Bd. 43, Nr. 3, pp. 139-143, 2002.

[7] L. De Chiffre, S. Carmignato, J.-P. Kruth, R. Schmitt und A. Weckenmann, „Industrial applications of computed tomography," *CIRP Annals-Manufacturing Technology,* Bd. 63, Nr. 2, pp. 655-677, 2014.

[8] A. Cantatore und P. Müller, „Introduction to computed tomography," 2011.

[9] A. Reh, B. Plank, J. Kastner, E. Gröller und C. Heinzl, „Porosity Maps--Interactive Exploration and Visual Analysis of Porosity in Carbon Fiber Reinforced Polymers," in *Computer Graphics Forum,* 2012.

[10] A. Reh, C. Gusenbauer, J. Kastner, M. E. Gröller und C. Heinzl, „MObjects--A Novel Method for the Visualization and Interactive Exploration of Defects in Industrial XCT Data," *Visualization and Computer Graphics, IEEE Transactions on,* Bd. 19, Nr. 12, pp. 2906-2915, 2013.

[11] G. Rao, B. Plank und J. Kastner, „Comparison of different segmentation methods for porosity evaluation in CFRP-reference samples with real porosity samples," *6th Conference on Industrial Computed Tomography,* 2016.

[12] Volume Graphics GmbH, „VGStudiomax 2.2," Heidelberg, Germany, 2013.

[13] C. Heinzl, A. Reh, M. Arikan, J. Weissenböck, A. Amirkhanov, B. Fröller, W. Li und M. Reiter, „iAnalyse 2.3," University of Applied Sciences Upper Austria Research and Development Limited, 2013.

Excerpt from ISBN 978-3-00-053387-7

[14] R. Stössel, D. Kiefel, R. Oster, B. Diewel und L. L. Prieto, „Computed Tomography for 3D Porosity Evaluation in Carbon Fibre Reinforced Plastics (CFRP),“ 2011.

[15] B. Plank, G. Rao und J. Kastner, „Evaluation of cfrp-reference samples for porosity made by drilling and comparison with industrial porosity samples by means of quantitative XCT.,“ 2015.

[16] B. Plank, J. Sekelja, G. Mayr und J. Kastner, „Porositätsbestimmung in der Flugzeugindustrie mittels Röntgen-Computertomografie,“ 2010.

[17] J. Kastner, B. Plank, D. Salaberger und J. Sekelja, „Defect and porosity determination of fibre reinforced polymers by X-ray computed tomography,“ in *2nd International Symposium on NDT in Aerospace*, 2010.

[18] N. Otsu, „A threshold selection method from gray-level histograms,“ *Automatica,* Bd. 11, Nr. 285-296, pp. 23-27, 1975.

Excerpt from ISBN 978-3-00-053387-7